Broad dispersion and lung localization of virus-specific memory B cells induced by influenza pneumonia

Hye Mee Joo, Yuxia He*, and Mark Y. Sangster†

Department of Microbiology, University of Tennessee, Knoxville, TN 37996

Communicated by Peter C. Doherty, University of Melbourne, Parkville, Victoria, Australia, January 1, 2008 (received for review December 2, 2007)

Although memory B cells (B_{Mem}) contribute significantly to resistance to infection, B_{Mem} population characteristics that may relate to protective efficacy have received little attention. Here, we report a comprehensive quantitative analysis of virus-specific IgG and IgA B_{Mem} dispersion after transient influenza pneumonia in mice. From early in the response, B_{Mem} circulated continuously and dispersed widely to secondary lymphoid tissues. However, a complicated picture emerged with B_{Mem} frequency differences between secondary lymphoid tissues indicating an influence of local tissue factors on trafficking. B_{Mem} numbers increased and stabilized at tissue-specific frequencies without contraction of the B_{Mem} pool during the period of analysis. The lung was notable as a nonsecondary lymphoid tissue where a rapid influx of IgG and IgA B_{Mem} established relatively high frequencies that were maintained long term. Our findings provide insights into the pattern of B_{Mem} dispersion, and emphasize the lung as a complex repository of immune memory after local infection.

antibody | infection | lymphocyte trafficking | respiratory tract | vaccination

Memory B and T cell subsets generated during adaptive immune responses play a key role in long-term resistance to infectious agents expressing previously encountered antigens. After formation in organized secondary lymphoid tissues, the cellular elements of immunological memory migrate by function-related trafficking pathways and populate lymphoid and non-lymphoid tissues throughout the body. This process establishes a dispersed state of cellular memory that optimizes protective efficacy. The dispersed CD4 and CD8 memory T cell populations have been well characterized (1–3), but similar comprehensive studies of B cell memory have not been performed (4).

The two cellular components of B cell memory, long-lived plasma cells (LLPCs) and memory B cells (B_{Mem}), are the products of germinal center reactions in secondary lymphoid tissue (5). LLPCs are classically recognized as Ab-secreting cells (ASCs) that localize in the bone marrow (BM) and maintain circulating Ab levels (6). However, long-lasting populations of IgA-secreting cells (in particular) are also established at mucosal surfaces after mucosal immunization where they provide local protection (7, 8). In contrast to plasma cells, B_{Mem} are quiescent cells that require stimulation to divide and differentiate into ASCs. On encounter with recall antigen, B_{Mem} mediate the rapid, vigorous, and high-affinity secondary Ab response that plays a key role in immune protection. The impression from studies to date is that B_{Mem} spread widely to organized lymphoid tissues (9–11), but the full extent of B_{Mem} dispersion has not been determined. It is also unclear whether B_{Mem} trafficking patterns relate to the Ab isotype expressed.

The present study provides a comprehensive quantitative analysis of the dispersed cellular components of B cell memory induced by influenza A virus infection. Intranasal (i.n.) influenza virus administration results in a highly localized pulmonary infection because of the dependence of viral replication on a trypsin-like enzyme that is largely restricted to respiratory epithelial cells (12). Although infected pulmonary dendritic cells are thought to travel to regional lymphoid tissues and spleen and drive influenza-specific T and B cell responses, little if any infectious virus is detected outside the lung (13–15). The development of adaptive immune responses correlates with the clearance of infectious virus from the lung, which is complete ≈10 days after infection (16, 17). The strong influenza-specific B cell response to infection is dominated by the production of IgG isotypes, but there is also a substantial IgA response. Thus, the model provides an opportunity to compare the state of both IgG and IgA memory. Our findings provide insights into the anatomically dispersed state of B cell memory established during the return to homeostasis after a transient, localized viral infection of the lung.

Results

The primary influenza-specific ASC response to i.n. administered virus has been well characterized. Initially, responses develop in the organized nasal-associated lymphoid tissues (o-NALT), which sample antigens in the upper respiratory tract, and in the cervical (CLN) and mediastinal (MedLN) lymph nodes, which drain the upper and lower respiratory tract, respectively (7, 18). A delayed response develops in the spleen, presumably reflecting the transit time of antigen-laden dendritic cells migrating from the lung. Responses in these sites wane rapidly after the elimination of infectious virus. The response kinetic values are notably different in the BM and in the submucosa of the upper and lower respiratory tract, where long-maintained populations of influenza-specific ASCs are established (7, 8, 19). To expand our understanding of B cell memory generated by primary influenza pneumonia, we determined the frequencies of virus-specific ASCs and B_{Mem} in a broad range of anatomical locations 8–12 wk after infection. At this time, a fully dispersed and stabilized state of B cell memory would be expected (10).

Tissue Distribution of Influenza-Specific IgG B_{Mem}. Influenza-specific IgG B_{Mem} were present in all of the organized lymphoid tissues examined (Fig. 1*A*). B_{Mem} frequencies expressed as a proportion of total cells were significantly higher in the o-NALT, MedLN, and Peyer's patches (PP) than in multiple other sites (Fig. 1*A*, legend). Interestingly, IgG B_{Mem} preferentially localized in the PP, even though influenza-specific ASCs were not generated at this site during the primary response to infection (data not shown). Notably, a relatively high B_{Mem} frequency was also present in the lung, a site of plasma cell concentration (Fig. 1*B*).

Author contributions: M.Y.S. designed research; H.M.J., Y.H., and M.Y.S. performed research; H.M.J. and M.Y.S. analyzed data; and M.Y.S. wrote the paper.

The authors declare no conflict of interest.

*Present address: Department of Immunology, St. Jude Children's Research Hospital, Memphis, TN 38105.

†To whom correspondence should be addressed. E-mail: msangste@utk.edu.

IMMUNOLOGY

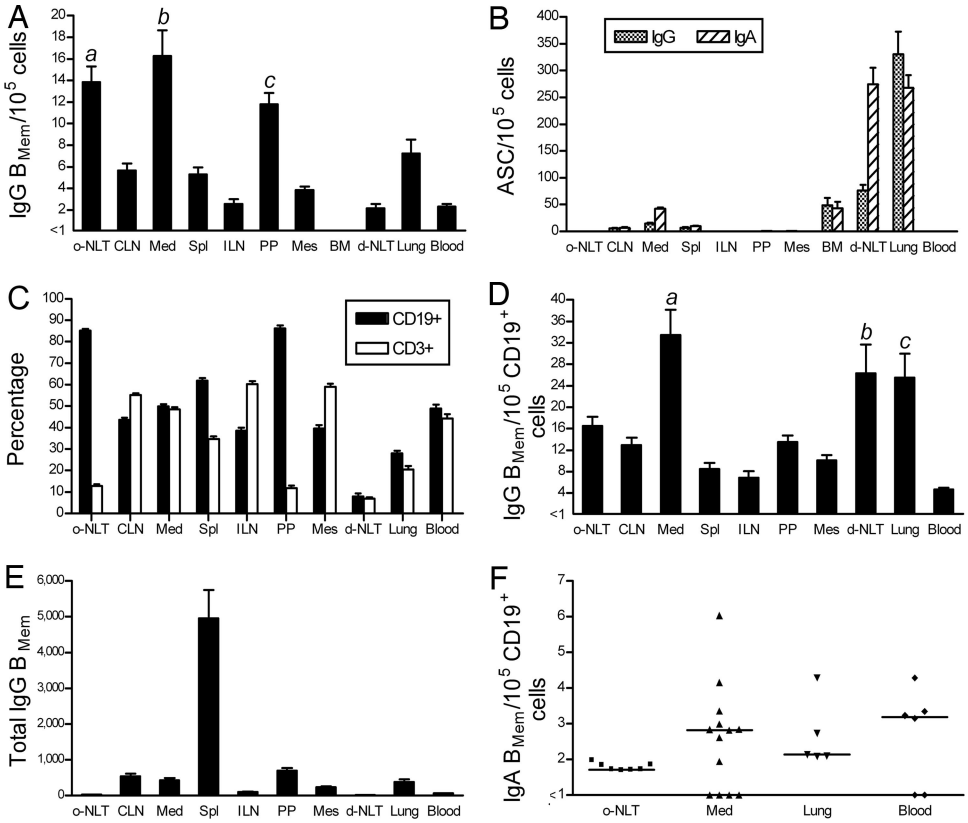

Fig. 1. Quantitative analysis of anatomically dispersed influenza-specific B_{Mem} and ASCs. Mice were sampled 8–12 wk after i.n. influenza infection. o-NLT, organized nasal-associated lymphoid tissue; CLN, cervical lymph node; Med, mediastinal lymph node; Spl, spleen; ILN, inguinal lymph node; PP, Peyer's patches; Mes, mesenteric lymph node; BM, bone marrow; d-NLT, diffuse nasal-associated lymphoid tissue. (*A*) IgG B_{Mem} frequencies expressed as a proportion of total cells. B_{Mem} frequencies (*A* and *F*) were determined by LDA based on *in vitro* stimulation of B_{Mem} to generate ASCs. Formation of IgG and IgA ASCs were taken to reflect precursor IgG and IgA B_{Mem}, respectively. $P < 0.0001$ for frequency differences among anatomical locations. (*a*) o-NLT vs. ILN, d-NLT, and blood ($P < 0.001$), and vs. CLN, Spl, and Mes ($P < 0.01$). (*b*) Med vs. CLN, Spl, ILN, Mes, d-NLT, lung, and blood ($P < 0.001$). (*c*) PP vs. ILN, d-NLT, and blood ($P < 0.05$). Data are mean + SEM ($n = 4$–6 for PP, Mes, BM, d-NLT, and blood; otherwise $n = 8$–12). (*B*) IgG and IgA ASCs were enumerated by direct *ex vivo* ELISPOT assay and are expressed as a proportion of total cells. Data are mean + SEM ($n = 5$–12). (*C*) Percentages of B cells (CD19$^+$) and T cells (CD3$^+$) were determined by flow cytometry. Data are mean + SEM ($n = 5$–12). (*D*) IgG B_{Mem} frequencies shown in *A* expressed as a proportion of CD19$^+$ cells. Data are mean + SEM. $P < 0.0001$ for frequency differences among anatomical locations. (*a*) Med vs. CLN, Spl, ILN, and blood ($P < 0.001$), vs. o-NLT and Mes ($P < 0.01$), and vs. PP ($P < 0.05$). (*b*) d-NLT vs. ILN and blood ($P < 0.01$), and vs. Spl ($P < 0.05$). (*c*) Lung vs. vs ILN and blood ($P < 0.01$), and vs. Spl ($P < 0.05$). (*E*) Total IgG B_{Mem} were calculated from the frequency (shown in *A*) and cell yield. Data are mean + SEM. (*F*) IgA B_{Mem} frequencies expressed as a proportion of CD19$^+$ cells. Only tissues that had measurable IgA B_{Mem} frequencies on at least one occasion are shown. The median of each group is indicated by a line. Frequencies were below the level of assay sensitivity in the following tissues ($n = 3$–5): CLN, Spl, ILN, PP, Mes, and BM. $P = 0.0004$ for frequency differences among all anatomical locations analyzed. IgA B_{Mem} frequencies were not significantly different in pairwise comparisons of anatomical locations.

The BM contained a substantial plasma cell population, but B_{Mem} were infrequent (<1 in 10^5) and may have been contaminating cells in the vasculature. B_{Mem} were consistently present in the blood, indicating maintenance of B_{Mem} circulation long after viral clearance.

There was a considerable range in the proportions of CD19$^+$ B cells in the different anatomical sites examined, with high percentages in the o-NALT and PP and low percentages in the diffuse(d)-NALT and lung (Fig. 1*C*). Enrichment and depletion experiments established that the CD19$^+$ population contained all of the influenza-specific B_{Mem} detected in our analysis (data not shown). Therefore, to standardize site-to-site comparisons, influenza-specific IgG B_{Mem} frequencies were calculated as a proportion of CD19$^+$ cells (Fig. 1*D*). This analysis clearly established anatomical differences in IgG B_{Mem} localization ($P < 0.0001$) and identified the MedLN, lung, and d-NALT as sites of preferential concentration. The proportion of IgG B_{Mem} in the CD19$^+$ cell population was significantly higher in the MedLN than in all other sites except the lung and d-NALT, and was significantly higher in the lung and d-NALT compared with the spleen, inguinal lymph node (ILN), and blood (Fig. 1*D*, legend). The prominence of the o-NALT and PP as sites of B_{Mem} localization (Fig. 1*A*) was less marked after standardizing the expression of B_{Mem} frequencies. With this adjustment, frequencies in the o-NALT and PP were still consistently higher than in the spleen and some lymph nodes, but differences were not statistically significant. B_{Mem} frequencies did not correlate with participation of the tissue in the immune response to influenza, as evidenced by significantly higher frequencies in the MedLN compared with the CLN (both responding sites), and similar frequencies in the CLN and nonresponding sites such as the PP and mesenteric lymph node (MesLN). The overall impression is one of widespread IgG B_{Mem} dispersion modulated by local tissue factors.

The total number of IgG B_{Mem} in each anatomical location was calculated from the frequency and cell yield (Fig. 1*E*). Because of its cellularity, the spleen was by far the major repository with ≈5,000 IgG B_{Mem}, representing close to two-thirds of the total IgG B_{Mem} measured in the analysis.

Tissue Distribution of Influenza-Specific IgA B_{Mem}. Influenza-specific IgA B_{Mem} frequencies differed depending on anatomical loca-

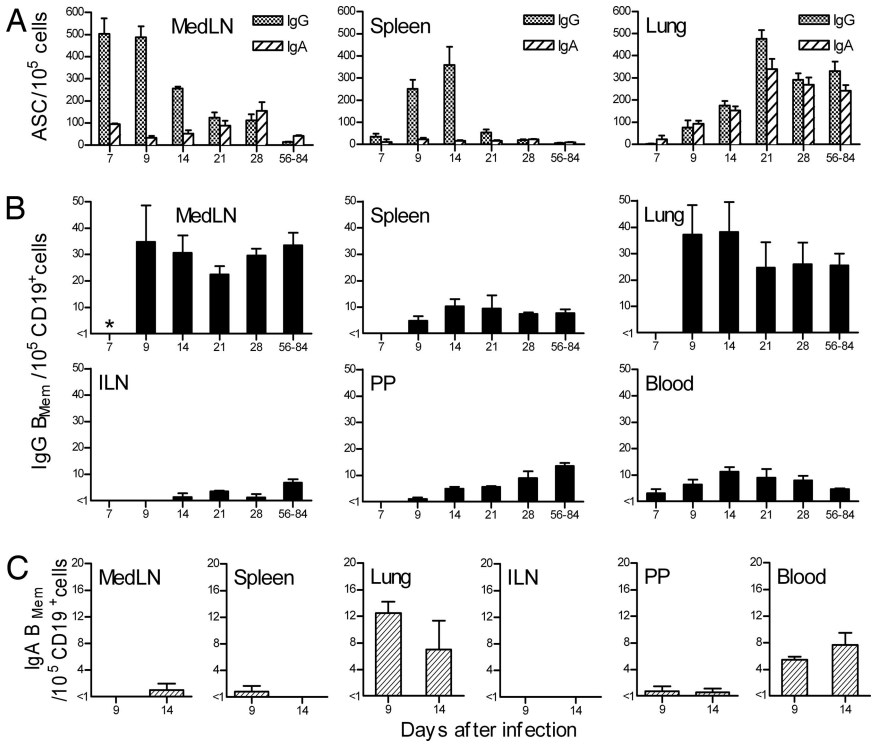

Fig. 2. Kinetic analysis of influenza-specific ASC and B_{Mem} generation and dispersion. Mice were sampled at intervals after i.n. influenza infection. Data for days 56–84 from the analysis shown in Fig. 1 are included for comparison. MedLN, mediastinal lymph node; ILN, inguinal lymph node; PP, Peyer's patches. (*A*) IgG and IgA ASC frequencies in the MedLN, spleen, and lung were enumerated by direct *ex vivo* ELISPOT assay and are expressed as a proportion of total cells. Data are mean + SEM (n = 3–7 for days 7–28). (*B*) IgG B_{Mem} frequencies in the MedLN, spleen, lung, ILN, PP, and blood expressed as a proportion of $CD19^+$ cells. Frequencies were determined by LDA based on *in vitro* stimulation of B_{Mem} to generate ASCs. Formation of IgG ASCs was taken to reflect precursor IgG B_{Mem}. Data are mean + SEM (n = 3 for days 7–28). *, the IgG B_{Mem} frequency in the responding MedLN on day 7 was >1 in 10^5 cells, but could not be accurately measured by LDA. (*C*) IgA B_{Mem} frequencies in the MedLN, spleen, lung, ILN, PP, and blood expressed as a proportion of $CD19^+$ cells. Frequencies were determined as for *B*, with formation of IgA ASCs taken to reflect precursor IgA B_{Mem}. Data are mean + range (n = 2).

tion (P = 0.0004) (Fig. 1*F*). Measurable IgA B_{Mem} frequencies were present in the majority of samplings in the o-NALT, MedLN, lung, and blood. In all other locations examined, frequencies were always below the level of sensitivity of the assay (frequency <1 in 10^5 cells). IgA B_{Mem} frequencies in the o-NALT, MedLN, and lung were approximately one-tenth of the IgG B_{Mem} frequencies, perhaps reflecting the overall IgA:IgG composition of the primary response to infection (Fig. 2*A*). The presence of IgA B_{Mem} in the blood suggests continuous recirculation, as was the case for IgG B_{Mem}.

Kinetics of Influenza-Specific AFC and B_{Mem} Generation and Dispersion. To gain insights into the establishment of the dispersed state of B cell memory, we determined influenza-specific ASC and B_{Mem} frequencies in selected sites at intervals after infection (Fig. 2). A vigorous IgG ASC response accompanied by B_{Mem} production developed first in the MedLN and later in the spleen (Fig. 2*A*). In contrast to the peak and decline in IgG ASC frequencies in the MedLN and spleen, the pattern for IgG B_{Mem} was the quick establishment and maintenance of the frequencies that were characteristic of these tissues in the long term (Fig. 2*B*). As early as day 7 after infection, the presence of circulating IgG B_{Mem} indicated that B_{Mem} dispersion from sites of generation had commenced. Notably, IgG B_{Mem} were detected in the lung as early as day 7 (<1 in 10^5 total cells) and had increased substantially in numbers by day 9, raising the possibility of a functional significance of these cells during the acute response. A limited analysis of IgA B_{Mem} on days 9 and 14 demonstrated circulating cells and relatively high frequencies in the lung, emphasizing the lung as a site of rapid and preferential B_{Mem} localization (Fig. 2*C*). ASC frequencies in the lung progressively increased from 1 to 3 wk after infection and then plateaued, a kinetic pattern consistent with the immigration of ASCs (and presumably also B_{Mem}) from other sites, rather than local synthesis. Although IgA ASCs were consistently present in the blood from 1 to 3 wk after infection (5–10 IgA ASC in 10^5 cells), circulating IgG ASCs were never detected, perhaps reflecting an influence of isotype expression on the differentiation rate of activated B cells. IgG B_{Mem} were detected earlier and established higher frequencies in the PP compared with the ILN, even though immune responses to influenza do not occur in either site. The general pattern was for IgG B_{Mem} frequencies in all tissues to increase and stabilize, with no evidence of contraction of the B_{Mem} pool during the period of analysis.

Discussion

The state of B cell memory generated by influenza infection of the respiratory tract provides profound and long-lasting resistance to reinfection with the homologous virus, and varying levels of protection against nonhomologous but serologically related strains. The protection provided by preexisting virus-specific Abs produced by ASCs in the upper and lower respiratory tract and in the BM is well recognized. However, much less attention has been given to the virus-specific B_{Mem} pool, even though this is likely to be of considerable importance in conferring long-term protection, especially if preexisting Ab levels begin to fall. The present analysis focuses on the virus-specific B_{Mem} population generated by primary influenza infection.

Our findings are consistent with the concept of widespread B_{Mem} dispersion to secondary lymphoid tissues throughout the

IMMUNOLOGY

body. However, what also emerge are significant tissue-specific influences on B_{Mem} localization. After adjusting for the proportion of $CD19^+$ cells, the MedLN, d-NALT, and lung stood out as sites of preferential IgG B_{Mem} localization. The high B_{Mem} frequency in the MedLN is not simply a consequence of a vigorous B cell response and B_{Mem} formation in this site, because the CLN also responds strongly to infection. Indeed, multiple site-to-site comparisons indicate that participation in the response to infection is not a determinant of the IgG B_{Mem} frequency that is established. IgG B_{Mem} frequencies in the o-NALT and PP, although significantly lower than in the MedLN, were still consistently higher than in the spleen and some lymph nodes, suggesting additional complexity in the regulation of B_{Mem} localization. The set of expressed homing molecules that direct B_{Mem} migration is not well established and may vary within the B_{Mem} population (20). Because naïve cells and B_{Mem} traffic through many of the same lymphoid tissues, there is likely to be considerable overlap in the homing molecules that regulate the process (21). However, even subtle differences between naïve and memory B cells in the expression levels of homing molecules may be sufficient to bias B_{Mem} localization. For example, up-regulation of $\alpha4\beta7$ on B_{Mem} (20) may favor entry into the PP, o-NALT, and mucosa-associated lymph nodes, where high endothelial venules (HEV) display relatively high levels of MadCAM-1, the $\alpha4\beta7$ ligand (22). Our findings may also reflect tissue differences in the rate of egress of lymphocytes. A key component of this process is receptor-mediated cell migration along an increasing sphingosine-1-phosphate (S1P) concentration gradient between the lymphoid tissue interior and adjacent blood or lymph (23). Inflammatory mediators released early in immune responses stimulate local overproduction of S1P in lymphoid tissues, leading to disruption of the S1P concentration gradient or down-regulation of cell receptors for S1P. The result is a transient block in lymphocyte egress from lymphoid tissues. Thus, high B_{Mem} frequencies in constitutively active lymphoid tissues like the PP and o-NALT may be a consequence of both preferential entry and delayed egress.

Importantly, our studies demonstrate that a relatively high frequency of virus-specific IgG B_{Mem} is established and maintained in the lung after influenza infection. This finding emphasizes the complexity of the lung as a site for the localization of the cellular elements of adaptive immunity. Previous studies have established that virus-specific ASCs and memory $CD4^+$ and $CD8^+$ T cells persist in the lung long after influenza and other viruses that target the respiratory tract have been cleared (8, 24–26). The kinetics of B_{Mem} (and ASC) movement into the lung resembled that reported for virus-specific $CD4^+$ and $CD8^+$ T cells (27–29). There is little information on molecules specifically expressed by B_{Mem} that direct entry into the lung, but at least initially the process is likely to resemble that for activated lymphocytes, in general, as they exit the vasculature in response to local inflammation-associated changes (30, 31). Up-regulation of $\alpha4\beta1$ on B_{Mem} may be expected, because the $\alpha4\beta1$/VCAM-1 adhesion pathway is a key element in lymphocyte trafficking into the inflamed lung (32). The microanatomical location of B_{Mem} in the lung has not been identified, but they may come to reside primarily in the relatively organized regions of lymphoid tissue that form in lung within 10 days of infection (33). This lymphoid tissue, collectively referred to as induced bronchus-associated lymphoid tissue (BALT), includes areas that resemble secondary lymphoid tissue with distinct B and T cell zones and HEV. Lymphocyte homing to BALT, as well as to PP and peripheral lymph nodes, highly depends on L-selectin and LFA-1 expression (34). However, the BALT-homing pathway may rely particularly on $\alpha4\beta1$/VCAM-1 interactions, because VCAM-1 is expressed at much higher levels on BALT HEV than on HEV in other secondary lymphoid tissues (34). T cell studies indicate that lung lymphocytes are part of a recirculating pool (35), moving by lymphatics through draining lymph nodes to eventually reach the venous blood. A preferential lymphocyte trafficking circuit from lung $\rightarrow$ draining lymph nodes $\rightarrow$ blood $\rightarrow$ lung has been proposed (36), and may underlay the high B_{Mem} frequencies that we consistently observed in the MedLN. The IgG B_{Mem} frequency (as a proportion of $CD19^+$ cells) was also relatively high in the d-NALT sample, which consisted of cells isolated from the thin tissue lining the nasal cavity (o-NALT excluded). This result reflects the presence of a small number of B_{Mem} in a tissue that contained few lymphocytes.

Influenza-specific IgG B_{Mem} frequencies in the BM were always below the level of sensitivity of the assay (<1 in 10^5 cells), in contrast to the concentration of LLPCs in this site. Our findings are consistent with other studies that reported the scarcity of B_{Mem} in the BM (9, 10). Interestingly, this contrasts with the role of the BM as a significant reservoir of memory T cells (1, 37). Although distinct trafficking characteristics may contribute to the difference between memory T and B cell frequencies in the BM (38), another factor may be B_{Mem} differentiation in the BM microenvironment to replenish the LLPC population.

Only the o-NALT, MedLN, lung, and blood had measurable influenza-specific IgA B_{Mem} frequencies when analyzed 8 wk or more after infection. This finding may simply reflect a consistent ratio of IgG:IgA B_{Mem} ($\approx$10:1) in all of the solid tissues sampled, because this could result in IgA B_{Mem} frequencies below the level of assay sensitivity in all sites except the o-NALT, MedLN, and lung. Alternatively, our data can be taken to reflect preferential IgA B_{Mem} trafficking to the respiratory tract and associated lymphoid tissues. It is well established that the expression of different sets of adhesion molecules and homing receptors by IgG- and IgA-producing ASCs results in preferential trafficking to the BM and mucosal sites, respectively (39). There is evidence for further compartmentalization of IgA ASC trafficking, with preferential migration to either the small intestine or to other mucosal sites like the lung (40). Further studies are required to firmly establish whether an analogous situation applies to IgA B_{Mem}. Our analysis demonstrated a rapid increase in IgA B_{Mem} frequency in the lung during the acute response, with maintenance of a lower frequency in the long term. In contrast, IgA B_{Mem} frequencies in the MedLN (presumably a key site of IgA B_{Mem} formation) stabilized at higher frequencies after clearance of the virus. This may reflect the lymphocyte-trafficking pathway from lung to draining lymph nodes discussed earlier.

In our analysis of the MedLN and spleen, long-term B_{Mem} frequencies (per total cells) were comparable to previous limiting dilution assay (LDA) determinations of memory $CD4^+$ and $CD8^+$ T cell frequencies (41, 42), although more recent studies (for example, using tetramers) indicate that the $CD8^+$ T cell frequencies may be somewhat higher (25, 43). A more dramatic difference exists in the lung; at least when comparing memory B and $CD8^+$ T cell frequencies (and numbers). During the memory phase after a primary infection, influenza-specific $CD8^+$ T cell numbers in the lung may exceed our estimate of B_{Mem} numbers by up to 100-fold (25, 27). This difference may be much less marked for memory $CD4^+$ T cells, which decrease in frequency in the lung much more rapidly than do $CD8^+$ T cells after viral clearance (28). A stable population of $\approx$30,000 influenza-specific ASCs was maintained in the lung after infection. These cells, which can be considered the effector form of B_{Mem}, are numerically more comparable with the memory $CD8^+$ T cell population in the lung. It is not known whether our LDA strategy underestimates influenza-specific B_{Mem} frequencies, as was shown to be the case for LDA analysis of $CD8^+$ T cell frequencies before the introduction of tetramers. However, at present, our approach may be the best option for enumerating a B_{Mem} population representing specificities for multiple, often poorly defined epitopes on different molecules.

In summary, the current report provides the most comprehensive picture currently available of the dispersed virus-specific B_{Mem} pool generated by primary influenza infection. Perhaps primarily, our findings focus attention on the lung as a complex repository of B and T cell memory that may contribute substantially to resistance to respiratory infections. The concept of effector lymphoid tissue (ELT) has been introduced to describe the stable accumulations of functionally significant memory T cells that are established in nonlymphoid tissues as a consequence of infection (44). Our studies demonstrate that B_{Mem} (as well as ASCs) should be recognized as components of the ELT that develop in the lung after influenza infection. Future studies are required to relate B_{Mem} numbers, location, and isotype expression to protective immunity and may have important implications for vaccine development.

Methods

Mice and Infection. C57BL/6J mice purchased from The Jackson Laboratory were housed under specific pathogen-free conditions until infection, and thereafter in BSL2 containment. Female mice were used in all experiments and were infected at 8–10 wk of age. Influenza virus A/HKx31 (H3N2) was grown in the allantoic cavity of embryonated hen's eggs. Mice were anesthetized with Avertin (2,2,2-tribromoethanol) given i.p., and then infected i.n. with $10^{6.8}$ 50% egg infectious doses of influenza virus (30 μl in Dulbecco's PBS). Animal procedures were approved by the Animal Care and Use Committee of the University of Tennessee.

Tissue Sampling and Treatment. Tissues collected from exsanguinated mice were processed to generate single-cell suspensions in IMDM (Invitrogen) containing L-glutamine (2 mM), sodium pyruvate (1 mM), penicillin (100 IU/ml), streptomycin (100 μg/ml), gentamicin (10 μg/ml), and 5×10^{-5} M β-mercaptoethanol (designated B cell medium, BCM), and supplemented with 10% FBS. Lymph nodes (CLN, MedLN, ILN, and MesLN) and spleen were disrupted between the frosted ends of microscope slides. BM cell suspensions were obtained by flushing the femurs and tibiae. Red blood cells were removed from the spleen and BM preparations by ammonium chloride lysis. Cell populations from the o-NALT and d-NALT were collected as described in ref. 45. Lungs were finely minced and incubated for 1 h at 37°C in BCM containing 10% FBS and 4 mg/ml collagenase type II (Worthington). Cells pelleted from the lung digest were resuspended in 40% isotonic Percoll and layered over 75% isotonic Percoll. After centrifugation at $600 \times g$ for 20 min at 25°C, cells at the interface were collected and washed. PP were dissected from the small intestine and washed, and cells were released by digestion with 2 mg/ml collagenase type I (Worthington) for 30 min at 37°C. Cells from heparinized blood were collected over Lympholyte-Mammal (Cedarlane) according to the manufacturer's instructions. Spleens were processed individually; otherwise tissues were pooled from two to five mice to generate sufficient cells for analysis. Cell populations were characterized by flow cytometry by using FITC-conjugated mAb to CD3ε (145-2C11) and PE-conjugated mAb to CD19 (1D3; BD Biosciences) as staining reagents.

Cell Enrichment. $CD19^+$ B cells were enriched (purity >95%) from single-cell suspensions by MACS by using murine CD19 MicroBeads and LS columns according to the manufacturer's instructions (Miltenyi Biotec).

ELISPOT Assay. Influenza-specific ASCs were enumerated by ELISPOT assay as described in ref. 46. Plate-bound secreted Abs were detected by using alkaline phosphatase-conjugated goat anti-mouse Abs with specificity for IgG or IgA (Southern Biotechnology).

Memory B Cell Assay. Influenza-specific B_{Mem} frequencies were determined by a previously described LDA based on *in vitro* stimulation of B_{Mem} to differentiate into ASCs (46). In brief, twofold dilutions of cells were incubated in 96-well tissue culture plates (routinely 12 wells per dilution), together with 10^6 irradiated (3,000 rad) syngeneic naïve spleen cell feeders plus β-propiolactone-inactivated HKx31 (Charles River). After incubation, cells in each well were transferred to ELISPOT plates for the enumeration of influenza-specific IgG or IgA ASCs. Preexisting virus-specific ASC numbers at the time of sampling were determined by direct *ex vivo* ELISPOT assay. After *in vitro* B_{Mem} activation and ELISPOT analysis, individual wells were scored positive for virus-specific B_{Mem} if progeny ASC numbers were greater than twice the mean preexisting ASC. The approach was modified for tissues that had high numbers of virus-specific ASCs at the time of sampling. For analysis of BM and d-NALT, wells were scored positive for B_{Mem} relative to unstimulated cultures (without inactivated-HKx31). Lung cell suspensions prepared 3 wk or more after infection were enriched for $CD19^+$ cells to reduce ASC numbers before *in vitro* stimulation, and were compared with unstimulated cultures for identification of positive wells. The virus-specific B_{Mem} frequency was calculated from the number of negative wells per cell dilution by extrapolation to the dilution that gave 37% negative wells (47). Linearity between the proportion of negative cultures and the input cell dose indicated direct measurement of B_{Mem}. Virus-specific IgG and IgA B_{Mem} were defined as cells that generated IgG and IgA ASCs, respectively, after *in vitro* stimulation (48, 49). No influenza-specific IgG or IgA ASCs were detected after *in vitro* stimulation of spleen, lung, or PP lymphocytes from naïve mice or from mice infected i.n. 8 wk previously with an unrelated virus (murine gammaherpesvirus 68). IgG and IgA B_{Mem} frequencies (per $CD19^+$ cells) in the lung were similar regardless of whether total or CD19-enriched immune cell populations were analyzed, indicating that results were independent of tissue-specific non-B cell factors (50). This was supported by a B_{Mem} analysis of CD19-enriched immune spleen cells stimulated in the presence of CD19-depleted immune PP cells, or CD19-enriched immune PP cells stimulated in the presence of CD19-depleted immune spleen cells (data not shown).

Statistical Analysis. Mean values were analyzed by using one-way ANOVA and the Tukey post test for multiple comparisons. The nonparametric Kruskal–Wallis test and Dunn's post test were used as required to accommodate values below the limit of assay sensitivity. Tests were performed by using GraphPad software. Values of $P < 0.05$ were considered statistically significant.

ACKNOWLEDGMENT. This work was supported by National Institutes of Health Grant AI061709 (to M.Y.S.).

1. Marshall DR, *et al.* (2001) Measuring the diaspora for virus-specific $CD8^+$ T cells. *Proc Natl Acad Sci USA* 98:6313–6318.
2. Reinhardt RL, Khoruts A, Merica R, Zell T, Jenkins MK (2001) Visualizing the generation of memory CD4 T cells in the whole body. *Nature* 410:101–105.
3. Masopust D, Vezys V, Marzo AL, Lefrancois L (2001) Preferential localization of effector memory cells in nonlymphoid tissue. *Science* 291:2413–2417.
4. Anderson SM, Tomayko MM, Shlomchik MJ (2006) Intrinsic properties of human and murine memory B cells. *Immunol Rev* 211:280–294.
5. McHeyzer-Williams LJ, McHeyzer-Williams MG (2005) Antigen-specific memory B cell development. *Annu Rev Immunol* 23:487–513.
6. Slifka MK, Ahmed R (1996) Long-term humoral immunity against viruses: Revisiting the issue of plasma cell longevity. *Trends Microbiol* 4:394–400.
7. Liang B, Hyland L, Hou S (2001) Nasal-associated lymphoid tissue is a site of long-term virus-specific antibody production following respiratory virus infection of mice. *J Virol* 75:5416–5420.
8. Jones PD, Ada GL (1986) Influenza virus-specific antibody-secreting cells in the murine lung during primary influenza virus infection. *J Virol* 60:614–619.
9. Bachmann MF, Kundig TM, Odermatt B, Hengartner H, Zinkernagel RM (1994) Free recirculation of memory B cells versus antigen-dependent differentiation to antibody-forming cells. *J Immunol* 153:3386–3397.
10. Slifka MK, Antia R, Whitmire JK, Ahmed R (1998) Humoral immunity due to long-lived plasma cells. *Immunity* 8:363–372.
11. Vanitha DJ, Joo HM, Rouse BT, Sangster MY (2007) Quantitative analysis of herpes simplex virus type 1-specific memory B cells generated by different routes of infection. *Virology* 360:136–142.
12. Steinhauer DA (1999) Role of hemagglutinin cleavage for the pathogenicity of influenza virus. *Virology* 258:1–20.
13. Eichelberger MC, Wang ML, Allan W, Webster RG, Doherty PC (1991) Influenza virus RNA in the lung and lymphoid tissue of immunologically intact and CD4-depleted mice. *J Gen Virol* 72:1695–1698.
14. Hamilton-Easton A, Eichelberger M (1995) Virus-specific antigen presentation by different subsets of cells from lung and mediastinal lymph node tissues of influenza virus-infected mice. *J Virol* 69:6359–6366.
15. Legge KL, Braciale TJ (2003) Accelerated migration of respiratory dendritic cells to the regional lymph nodes is limited to the early phase of pulmonary infection. *Immunity* 18:265–277.
16. Gerhard W, Mozdzanowska K, Furchner M, Washko G, Maiese K (1997) Role of the B-cell response in recovery of mice from primary influenza virus infection. *Immunol Rev* 159:95–103.
17. Woodland DL (2003) Cell-mediated immunity to respiratory virus infections. *Curr Opin Immunol* 15:430–435.
18. Sangster MY, *et al.* (2003) An early $CD4^+$ T cell-dependent immunoglobulin A response to influenza infection in the absence of key cognate T-B interactions. *J Exp Med* 198:1011–1021.
19. Hyland L, Sangster M, Sealy R, Coleclough C (1994) Respiratory virus infection of mice provokes a permanent humoral immune response. *J Virol* 68:6083–6086.
20. Roy MP, Kim CH, Butcher EC (2002) Cytokine control of memory B cell homing machinery. *J Immunol* 169:1676–1682.
21. Rodrigo MJ, von Andrian UH (2006) Specificity and plasticity of memory lymphocyte migration. *Curr Top Microbiol Immunol* 308:83–116.

22. Csencsits KL, Jutila MA, Pascual DW (1999) Nasal-associated lymphoid tissue: Phenotypic and functional evidence for the primary role of peripheral node addressin in naive lymphocyte adhesion to high endothelial venules in a mucosal site. *J Immunol* 163:1382–1389.
23. Cyster JG (2005) Chemokines, sphingosine-1-phosphate, and cell migration in secondary lymphoid organs. *Annu Rev Immunol* 23:127–159.
24. Hogan RJ, *et al.* (2001) Protection from respiratory virus infections can be mediated by antigen-specific $CD4^+$ T cells that persist in the lungs. *J Exp Med* 193:981–986.
25. Hogan RJ, *et al.* (2001) Activated antigen-specific $CD8^+$ T cells persist in the lungs following recovery from respiratory virus infections. *J Immunol* 166:1813–1822.
26. Ostler T, Hussell T, Surh CD, Openshaw P, Ehl S (2001) Long-term persistence and reactivation of T cell memory in the lung of mice infected with respiratory syncytial virus. *Eur J Immunol* 31:2574–2582.
27. Lawrence CW, Ream RM, Braciale TJ (2005) Frequency, specificity, and sites of expansion of $CD8^+$ T cells during primary pulmonary influenza virus infection. *J Immunol* 174:5332–5340.
28. Cauley LS, *et al.* (2002) Cutting edge: Virus-specific $CD4^+$ memory T cells in nonlymphoid tissues express a highly activated phenotype. *J Immunol* 169:6655–6658.
29. Roman E, *et al.* (2002) CD4 effector T cell subsets in the response to influenza: Heterogeneity, migration, and function. *J Exp Med* 196:957–968.
30. Luster AD, Alon R, von Andrian UH (2005) Immune cell migration in inflammation: Present and future therapeutic targets. *Nat Immunol* 6:1182–1190.
31. Kim CH (2004) Chemokine-chemokine receptor network in immune cell trafficking. *Curr Drug Targets Immune Endocr Metabol Disord* 4:343–361.
32. Feng CG, *et al.* (2000) Up-regulation of VCAM-1 and differential expansion of β integrin-expressing T lymphocytes are associated with immunity to pulmonary *Mycobacterium tuberculosis* infection. *J Immunol* 164:4853–4860.
33. Moyron-Quiroz JE, *et al.* (2004) Role of inducible bronchus associated lymphoid tissue (iBALT) in respiratory immunity. *Nat Med* 10:927–934.
34. Xu B, *et al.* (2003) Lymphocyte homing to bronchus-associated lymphoid tissue (BALT) is mediated by L-selectin/PNAd, $\alpha_4\beta_1$ integrin/VCAM-1, and LFA-1 adhesion pathways. *J Exp Med* 197:1255–1267.
35. Moyron-Quiroz JE, *et al.* (2006) Persistence and responsiveness of immunologic memory in the absence of secondary lymphoid organs. *Immunity* 25:643–654.
36. Zammit DJ, Turner DL, Klonowski KD, Lefrancois L, Cauley LS (2006) Residual antigen presentation after influenza virus infection affects CD8 T cell activation and migration. *Immunity* 24:439–449.
37. Di Rosa F, Pabst R (2005) The bone marrow: A nest for migratory memory T cells. *Trends Immunol* 26:360–366.
38. Mazo IB, *et al.* (2005) Bone marrow is a major reservoir and site of recruitment for central memory $CD8+$ T cells. *Immunity* 22:259–270.
39. Cyster JG (2003) Homing of antibody secreting cells. *Immunol Rev* 194:48–60.
40. McDermott MR, Bienenstock J (1979) Evidence for a common mucosal immunologic system. I. Migration of B immunoblasts into intestinal, respiratory, and genital tissues. *J Immunol* 122:1892–1898.
41. Topham DJ, Tripp RA, Hamilton-Easton AM, Sarawar SR, Doherty PC (1996) Quantitative analysis of the influenza virus-specific $CD4^+$ T cell memory in the absence of B cells and Ig. *J Immunol* 157:2947–2952.
42. Tripp RA, Sarawar SR, Doherty PC (1995) Characteristics of the influenza virus-specific $CD8^+$ T cell response in mice homozygous for disruption of the *H-2IA*^{b} gene. *J Immunol* 155:2955–2959.
43. Flynn KJ, *et al.* (1998) Virus-specific $CD8^+$ T cells in primary and secondary influenza pneumonia. *Immunity* 8:683–691.
44. van Panhuys N, Perret R, Prout M, Ronchese F, Le Gros G (2005) Effector lymphoid tissue and its crucial role in protective immunity. *Trends Immunol* 26:242–247.
45. Asanuma H, *et al.* (1997) Isolation and characterization of mouse nasal-associated lymphoid tissue. *J Immunol Methods* 202:123–131.
46. Li X, *et al.* (2006) A strategy for selective, $CD4^+$ T cell-independent activation of virus-specific memory B cells for limiting dilution analysis. *J Immunol Methods* 313:110–118.
47. Topham DJ, Doherty PC (1998) Longitudinal analysis of the acute Sendai virus-specific $CD4^+$ T cell response and memory. *J Immunol* 161:4530–4535.
48. Coffman RL, Cohn M (1977) The class of surface immunoglobulin on virgin and memory B lymphocytes. *J Immunol* 118:1806–1815.
49. Okumura K, Julius MH, Tsu T, Herzenberg LA, Herzenberg LA (1976) Demonstration that IgG memory is carried by IgG-bearing cells. *Eur J Immunol* 6:467–472.
50. Mora JR, *et al.* (2006) Generation of gut-homing IgA-secreting B cells by intestinal dendritic cells. *Science* 314:1157–1160.